ANALYSES OF JOVIAN DECAMETRIC RADIATION *S*-BURSTS INTERACTING WITH *N*-BURSTS

MASARU OYA
Geophysical Institute, Tohoku University

HIROSHI OYA
Fukui University of Technology

TAKAYUKI ONO and MASAHIDE IIZIMA
Geophysical Institute, Tohoku University

(Received 22 March 2001; Accepted 7 May 2002)

Abstract. Dynamic spectra of *S*-bursts of Jovian decametric radiations are obtained by using a high time resolution radio spectrograph which has a time resolution of 2 msec and the bandwidth of 2 MHz. Within occurrence of 65 *S*-burst events observed in the period from 1983 to 1999, 26 events have been identified as the *S*-*N* burst events, which are characterized by the interaction between the *S*-burst emissions and the Narrow band emissions. In the dynamic spectra of the *S*-*N* burst, the trend of emissions with negative and slower frequency drift named as "Trailing Edge Emission" are often observed shortly after the appearance of the *S*-burst. Detailed analyses of these phenomena revealed that the Trailing Edge Emission is not a manifestation of *S*-burst with slower drift rate but a variation of *N*-burst. The results suggested that *S*-burst and the associated Trailing Edge Emission are formed simultaneously started from a common region with different drift rates. It has been further suggested that the appearance of the *S*-bursts is not controlled by the geometrical effect between the source region and the observer, but directly reflects the generation of the source region widely distributed in an altitude range from a few thousands km to 30,000 km, along the Io flux tube.

Keywords: DAM, Jupiter, *N*-burst, *S*-burst, Tilted-V

1. Introduction

The *S*-bursts of the Jovian Decametric Radiation belong to a category of the shortest time duration phenomena, which show the rapid negative frequency drift during a few tens of milliseconds with the frequency drift rate ($\mathrm{d}f/\mathrm{d}t$) of a few tens of MHz/sec. In several proposed models, it has been widely accepted that an upward stream of bunched electron clouds generate the *S*-bursts approximately at the local electron gyrofrequency. There is a fundamental problem; what is the origin of these bunched electrons. Two possibilities of the location of the acceleration region of the bunched electrons have been proposed; i.e., one is near Io and the other is near the surface of Jupiter. Ellis (1975) has pointed out that the drift rates of *S*-bursts are generally increasing with increasing the frequency from 8 to 24 MHz. He has proposed a model of the formation of bunched electrons which are originally accelerated at Io; the bunched electrons are making bounce

Earth, Moon and Planets **88:** 187–209, 2002.

motions between the mirror points keeping a constant of the first adiabatic invariant (Ellis, 1975). The drift rates of *S*-bursts in a high frequency range over 24 MHz have further been studied by Desch et al. (1978), Riihimaa (1977, 1978, 1979), Krausche et al. (1976), Flagg and Desch (1979), Leblanc (1980b), Ellis (1982) and Boudjada et al. (1995). Their results unanimously showed that the drift rate of the *S*-burst increases with increasing the frequency even in a high frequency range. Their results are, then, contradictory to the model proposed by Ellis (1975), since the trapped electrons accelerated at Io are supposed to decrease the drift rates of the *S*-bursts in the high frequency range because of the mirror motion of electrons. Leblanc et al. (1980) has proposed another model of the acceleration of bunched electrons; the electrons are accelerated near the Jovian ionosphere along the field line with a direction of outward. The existence of such electrons can explain the observed trend of the drift rate of *S*-bursts (Leblanc et al., 1980). However, Zarka et al. (1996) have recently reported on the basis of their high frequency range observations over 32 MHz, that the dependence of drift rates on the frequency is different from previous results. Zarka et al. (1996) showed that the drift rate in the high frequency range rapidly decreases with the increment of the frequency. Then, their result supports the Ellis's model of trapped electrons which are accelerated at Io. Nevertheless this model is still subject of discussion as reported by Boudjada et al. (1996). They showed that the drift rate could not be fitted by only fixing the initial pitch angle and the electron speeds. These different observational results can be attributed to, the difficulty in the precise measurements of the drift rates due to the scarcity of *S*-burst occurrence in this high frequency range. Therefore, it has been still unknown where the electrons are accelerated.

In this paper we studied the origin of the *S*-bursts from the analyses of the interaction between *S*-bursts and *N*-bursts. The existence of *N*-bursts in the spectra of DAM emissions was found by Warwick (1963), Riihimaa (1964), and Warwick and Gordon (1965). *N*-bursts have been considered to belong to the category of the *L*-bursts although the *N*-burst has a restricted frequency range showing an almost constant frequency and a narrow band width. Carr et al. (1983) designated the narrow-band *L*-emissions as events of type N. Riihimaa (1985) reported statistical studies of the type of *N*-bursts.

The generation process of *N*-bursts is still unknown, too. In the case of the emissions in the Io-B sources, an *S*-burst occasionally makes an interaction with the *N*-burst. We call this interaction phenomenon between the *S*-burst and the *N*-burst as *S*-*N* burst event" (Riihimaa and Carr, 1981; Boudjada et al., 1995). In the dynamic spectra of *S*-*N* bursts, an *S*-burst appears as sloping line crossing a *N*-burst. At cross over point, there is a gap of *N*-burst emission with a substantial fraction of a second. Shortly after the appearance of the *S*-burst, the second trend of the negative frequency drift is generated with slower drift rate; this new trend has been called "Trailing Edge Emission" (Riihimaa and Carr, 1981). In the present report, we study the characteristics of the *S*-*N* burst event by using high-resolution spectra with the bandwidth of 2MHz. From the characteristics of the *S*-*N* burst, we

can obtain an important clue to seek for the possible generation mechanism of the *S*-bursts.

2. Observation

Observations of *S-N* bursts were made by using the high time resolution (2 msec) spectrograph with a band width of 2 MHz which had been originally developed by the group of Tohoku University in 1983. Since 1983, the high time resolution spectrograph was operated randomly in the Io-DAM region in the CML-Io diagram. The total observation time exceeds 600 h. The front-end of the system consists of orthogonally crossed log-periodic dipole antennas, a hybrid circuit for dividing received DAM signals into right-handed (RH) and left-handed (LH) polarization signals, and low noise wide-band pre-amplifiers. The log-periodic dipole antenna consists of 9 elements covering a frequency range from 20 MHz to 40 MHz was used for the present study.

The back end consists of two-stage super-heterodyne receiver and a video tape recorder to record DAM signals with band width of 2 MHz. This observation system records RH and LH signals alternately every 1/60 sec. The observation frequency can be selected within a range from 20 to 40 MHz by changing the 1st local oscillator frequency of the receiver. The recorded signals in VTR tape are reproduced and analyzed with a spectrum analyzer with a frequency resolution of 30 kHz and digitized with a 12 bits A/D converter unit.

An example of dynamic spectra of *S-N* bursts are shown in Figure 1 which shows a complicated interaction process of *S-N* bursts. To define the character of *S-N* bursts, the detail of dynamic spectra has been identified by using six parameters, as has been schematically illustrated in Figure 2. When a spectrum of *S*-burst interrupt with the trend of the *N*-burst, the *N*-burst disappears from the detectable range of the receiver. Shortly after the appearance of the *S*-burst, the second trend of emission appears showing slower frequency drift than that of the *S*-burst. The second emission is named as "Trailing Edge Emission" (hereafter abbreviated to "TEE"). When a TEE arrives to the frequency where the former *N*-burst was located, the TEE disappears, and *N*-burst appears again (see Figure 2). The periodic change (1/60 sec interval) of emissions in the dynamic spectra given in Figure 1 is caused by the observation gap due to the switching operation for the polarization measurement.

Among the observed 65 *S*-burst events from 1983 to 1999, 26 events have been identified as the *S-N* burst events. All of *S-N* burst events have been identified only in the Io-B region in the CML-Io phase diagram. In Figure 3, the occurrence probabilities of *L*-burst, *S*-burst and *S-N* burst in the Io-B region are plotted in the CML-Io phase diagram. As shown in this diagram, occurrence regions of *L*-burst and *S*-burst exclusively share the Io-B region. The occurrence region of the *L*-bursts forms inverted "*L*" shape taking region as if it avoids to appear in the

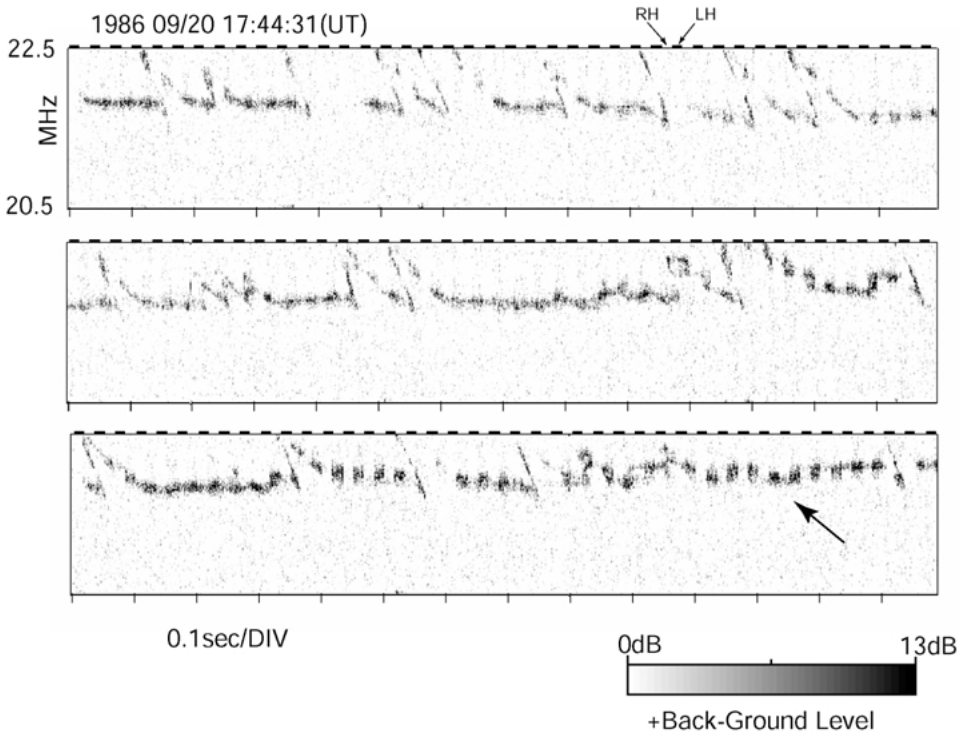

Figure 1. A typical example of dynamic spectrum of *S*-*N* bursts in a frequency range of 20.5 to 22.5 MHz. The observation was carried out from 17:44:31.0 to 17:44:35.2 (UT) on 20 September 1986. The periodic interruptions of emission which are indicated by arrow in this figure were caused by the recording system.

central part of Io-B region (centered at the Io phase of 80° and CML of 140°); the occurrence region of the *S*-burst appears in other part of Io-B region. These occurrence character of *L*-bursts and *S*-bursts is consistent with previous works by Riihimaa et al. (1970, 1981), Riihimaa (1978), Leblanc et al. (1980), Riihimaa and Carr (1981) and Boudjada et al. (1995). In Figure 3, we can find that the occurrence of the *S*-*N* bursts is located in the lower part of the occurrence region of the *S*-bursts, where occurrence of *S*-bursts has the highest probability. It has been still unknown why the occurrence regions of these three types of bursts show such distinct features in their distribution in the Io-B region; however, these features suggest that there is a interaction between the occurrences of *L*-bursts, *S*-bursts, and *S*-*N* bursts in the Io-B region and that these three types of emissions are not generated independently.

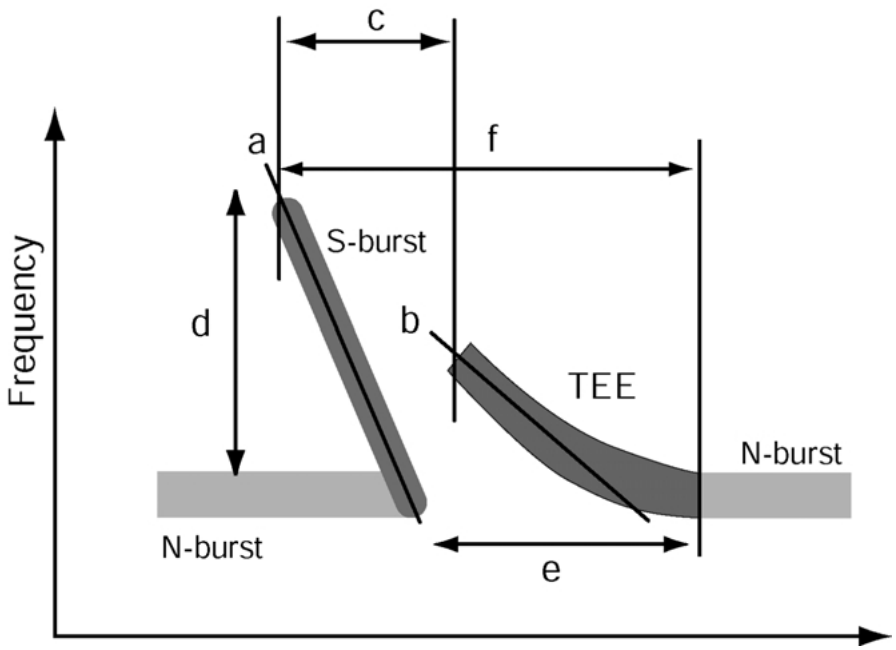

Figure 2. Definition of parameters. (a) *S*-burst drift rate (MHz/sec). (b) Trailing Edge Emission (TEE) drift rate (MHz/sec). (c) Delay Time from the appearance of *S*-burst (Time interval from the appearance of *S*-burst to the appearance of TEE). (d) *S*-burst Frequency Range (MHz). (e) Emission Gap (Interruptions interval *N*-burst) (msec). (f) Duration Time of a phenomenon (Time interval from the appearance of *S*-burst to the disappearance of TEE) (msec).

3. Characteristics of Trailing Edge Emission

As shown in Figure 2, an *S-N* burst has complex feature adding a new type emissions named "Trailing Edge Emission (TEE)" showing a interaction of *S*-bursts with *N*-bursts in the dynamic spectra. TEE appears just after the beginning of *S*-burst. The *N*-burst is interrupted within an time interval between the *S*-burst and the TEE as it has been indicated as "*e*" in Figure 2. The duration time of this phenomenon (from the appearance of the *S*-burst to end of TEE) is about 0.1 sec. In the previous works, the TEE was recognized as a kind of *S*-bursts because it has a similar falling tone spectra (Riihimaa and Carr, 1981). However, since the occurrence probability of TEEs is very small compared with other DAM emissions and it can only be observed by using the high-time-resolution dynamic spectrograph, the detailed characteristics of TEEs have not been well understood yet. Therefore, it has been still unsolved problem whether the TEEs belong to a category of *S*-bursts as suggested by Riihimaa and Carr (1981) or not. In this section, we analysis the basic characteristics of the TEEs to identify the nature of the TEE by using the 7 events above the observed 26 *S-N* burst events from 1983 to 1999. These 7 *S-N*

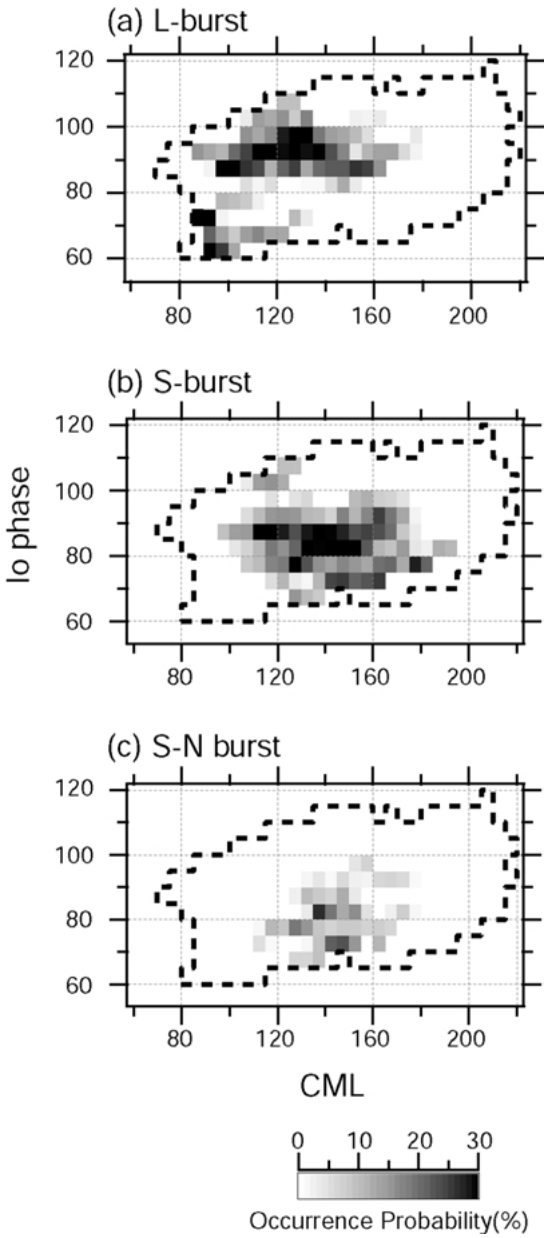

Figure 3. The occurrence probabilities of observed emissions in Io-B region. (a) *L*-burst. (b) *S*-burst. (c) *S-N* burst. The region surrounded by the dotted line shows the observed region.

burst events were quite intense and lasted for a long time, in which TEEs were displayed clearly.

3.1. RELATIONS BETWEEN *S*-BURST AND TEE

The TEE is characterized by a nature of falling tone forming *S*-burst-like dynamic spectra. However, it is clearly shows that the drift rates of the TEEs are lower than those of the *S*-bursts. In the panel (a) of Figure 4, occurrence numbers of corresponding bin of drift rates of *S*-bursts and TEEs are plotted. In this analysis, an uncertainty is estimated to be less than 2.5 MHz/sec for the measured drift rate of 30 MHz/sec, therefore, errors don't affect the observed occurrence number of drift rates. From this histogram, we can clearly find that the distributions of drift rates of *S*-bursts and TEEs are forming two groups. The average values of the drift rates of the *S*-bursts and the TEEs are about 25 MHz/sec and 10 MHz/sec, respectively. It is also clear by indicated that the range of the drift rate of TEE is narrower than that of *S*-burst. If the emission occurs instantaneously near the local electron cyclotron frequency, the negative frequency drift $\left(\frac{\mathrm{d}f}{\mathrm{d}t}\right)$ suggests that the generation region moves up from the Jovian ionosphere along the magnetic field line. The electron cyclotron frequency f is related to intensity of the local magnetic field B, as,

$$f = \frac{eB}{m_e}. \tag{1}$$

We assume that the magnetic field B of Jupiter is a dipole field in this study. Therefore, B can be expressed by

$$B(r, \theta) = B_E \left(\frac{1}{L}\right)^3 \frac{\sqrt{1 + 3\cos^2\theta}}{\sin^6\theta}, \tag{2}$$

where B_E is the magnetic field strength at the equator $B_E \simeq 4.2G$), L is the L value of Io ($\simeq 6$), r and θ are radical distance and the magnetic colatitude. Then, a relation between the drift rate $\mathrm{d}f/\mathrm{d}t$ and the electron cyclotron frequency f for electrons can be derived, as:

$$\frac{\mathrm{d}f}{\mathrm{d}t} = -\frac{3\cos\theta\sqrt{3 + 5\cos^2\theta}}{LR\sin^2\theta\sqrt{1 + 3\cos^2\theta}} V_d f, \tag{3}$$

where R_J indicates the Jovian radius ($R_J \simeq 71,372$ km) and V_d is the velocity of the generation region along the magnetic field line. In the panel (b) of Figure 4, the occurrence numbers are plotted for the velocity of the generation region for the same events as given in the panel (a), assuming that the magnetic field of Jupiter is a dipole field. The average velocities of the source region of *S*-bursts and TEEs are, respectively, about 30×10^6 m/sec (0.1c) and 15×10^6 m/sec (0.05c). Comparing the width of velocity range shown in Figure 4, the generation region of TEE moves

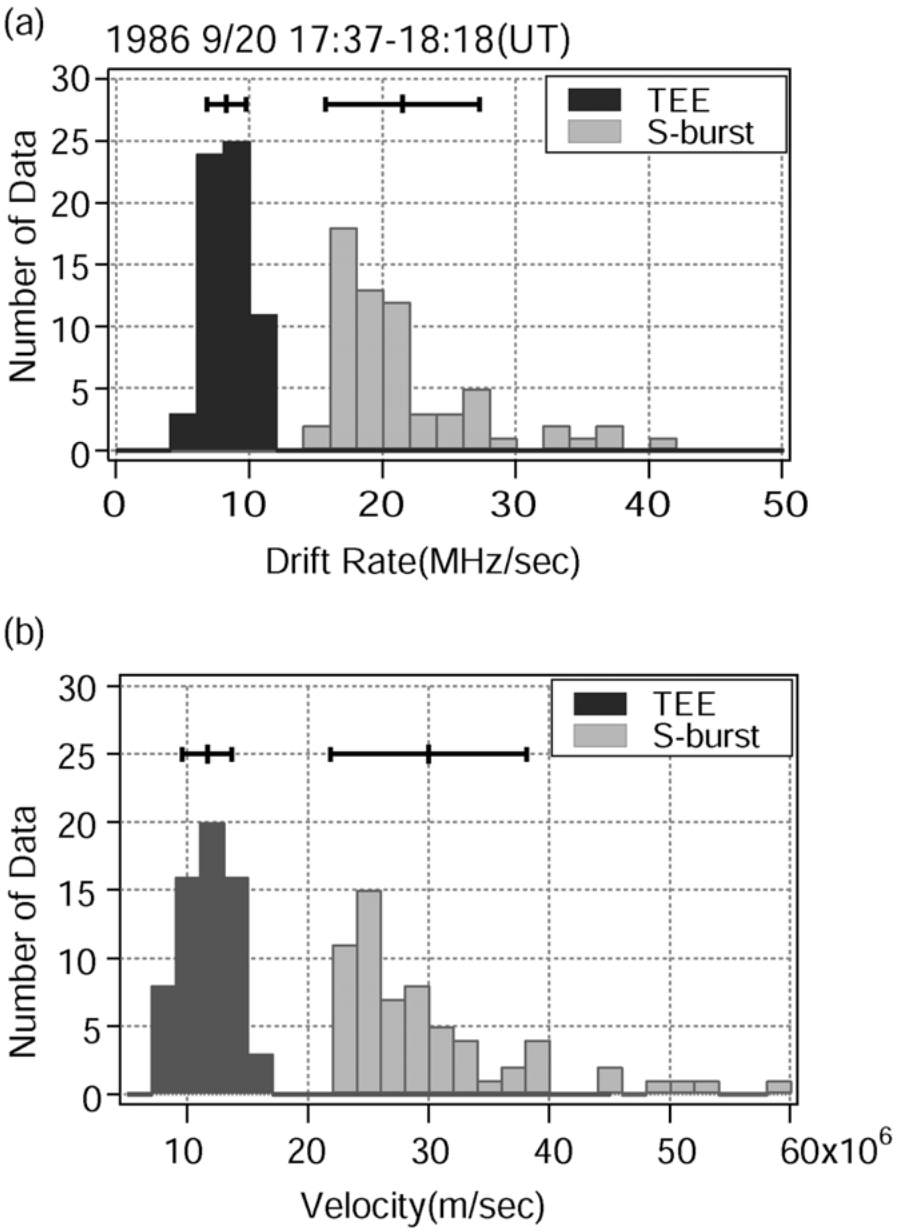

Figure 4. Distributions of drift rates and velocities of *S*-burst and TEE for the *S-N* burst event observed around 18h0m (UT) on 20 September 1986. The magnetic field is assumed to be a dipole field.

with relatively constant velocity in each event, while the traveling speed of *S*-burst is variable and distributes in wide range in Figure 4. This characteristic is shown in all 7 *S*-*N* burst events analyzed in this study (see Figures 6 and 7).

The correlation of drift rates between the pair of *S*-burst and TEE for each *S*-*N* burst events is interesting. In Figure 5, drift rates of the *S*-bursts are plotted versus those of associated TEEs for two events, 20 September 1986, 17:37–18:18 (UT) in panel (a) and 10 December 1989, 19:24–19:47 (UT) in panel (b). The uncertainties of individual measurements are indicated by error bars in the figures. As can be seen in Figure 5, there is no remarkable correlation between the drift rate of *S*-burst and that of the associated TEE. Further, the frequency dependence of the drift rates of *S*-bursts and the associated TEEs in the *S*-*N* events are indicated in Figure 6 for 7 *S*-*N* burst events, where the average drift rates of *S*-bursts and TEEs (indicated by solid and open marks) are plotted as a function of the observation frequency. Associated horizontal and vertical bars indicate the ranges of the deviation of the drift rates and the frequencies around their average values for each events. As mentioned in the introduction, the drift rate of *S*-burst changes depending on the observations frequency; the drift rate tends to increase with frequency, although the dependence in the high frequency range above 30 MHz is not clear. As can be seen in Figure 6, the drift rate of the *S*-burst measured in the *S*-*N* burst events has the same frequency dependence as a simple *S*-burst events. On the other hand, there is no clear dependence in the drift rates of TEEs. By using Equation (1), the velocity of the generation region along the magnetic field line has been estimated as a function of the frequency for both *S*-bursts and TEEs. The result is given in Figure 7 where the average velocities of generation region are plotted versus the emission frequency for the cases of *S*-bursts (panel (a)) and TEEs (panel (b)). As can be seen in the panel (a), averaged velocities of generation region of *S*-bursts show relatively small variance around the constant value of 24×10^6 m/sec (0.08c), while TEEs show different tendency as indicated in panel (b) where averaged velocities of TEEs show variety depending on the frequency of each event. On the other hand, in each event, deviation of flow velocities from the averaged value is much smaller than the case of *S*-bursts. It is noted that the flow velocity of generation region of TEE varies largely from one event to another.

In this section it has been shown that there is no correlation between the drift rates of the TEE and the associated *S*-burst. Although the mechanism controlling the motion of generation region of TEE is unknown, this result suggests that the generations mechanism of the TEE differs from that of the *S*-burst.

3.2. Relations between TEE and *N*-burst

As previously pointed out, typical *S*-*N* burst phenomena persist for only 0.1 sec from appearance of *S*-burst to the end of TEE; namely the *S*-*N* burst event is one of the shortest time-scale emission in DAMs. Figure 8 shows an example of *S*-*N* burst which was observed with high time resolution of 2 msec with a frequency

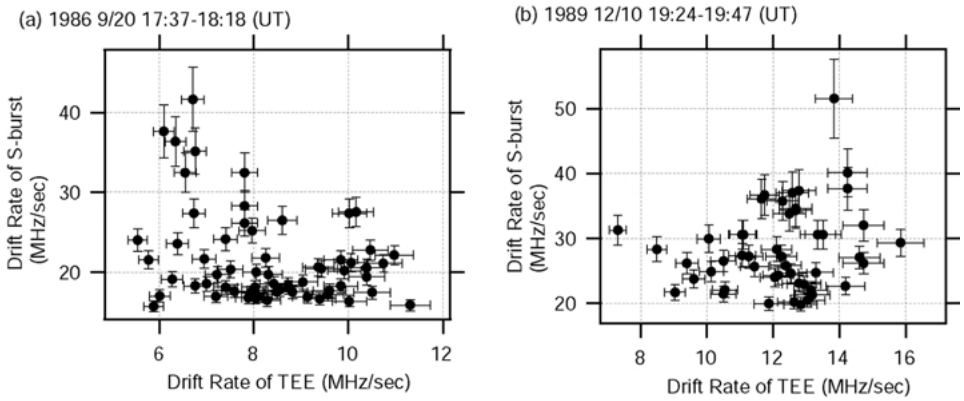

Figure 5. A diagram which shows the relation between the drift rates of *S*-burst and TEE. (a) The event observed around 18h0m (UT) on 20 September 1986. (b) The event observed around 19h30m (UT) on 10 December 1989.

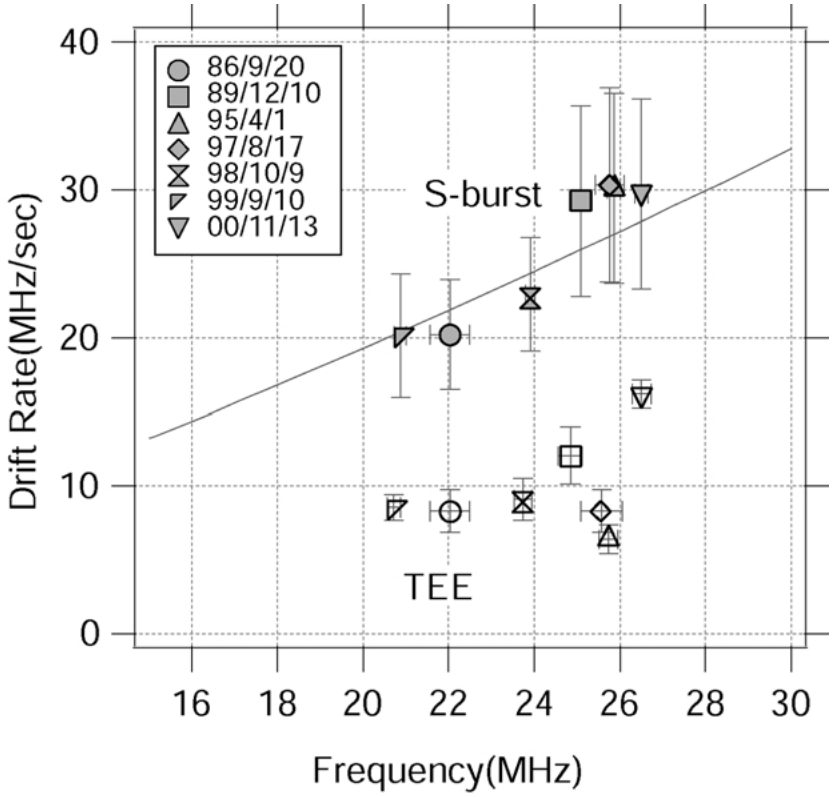

Figure 6. The frequency dependences of the average drift rates of *S*-bursts and TEEs in 7 *S*-*N* burst events. The associated horizontal and vertical bars are the dispersions of drift rate and frequency around their average values. The solid curves are calculated for the condition of the $V_d = 0.08c$.

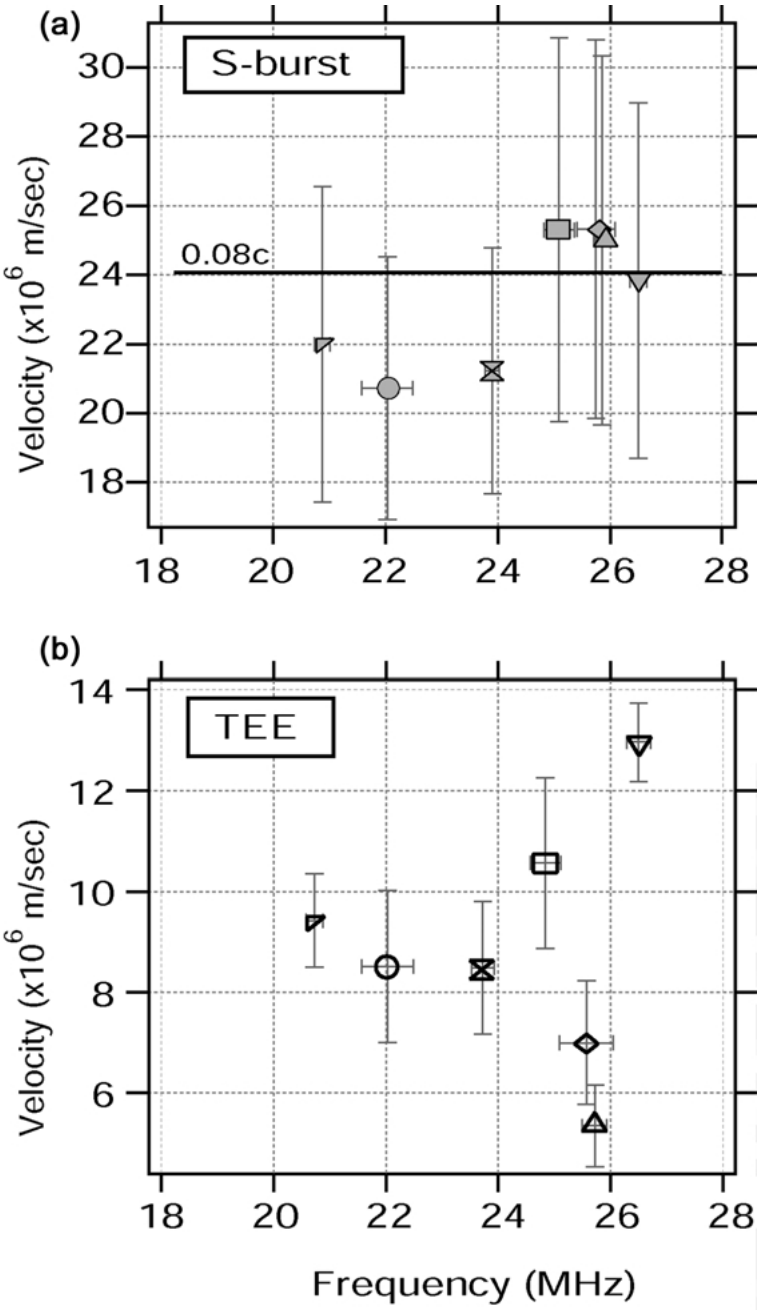

Figure 7. The frequency assumed dependence of the velocity of motion of generation regions along the magnetic field line. The magnetic field is assumed to be a dipole field. The format of marks is same as Figure 6. (a) Average velocity of generation regions of *S*-bursts. (b) Average velocity of generation regions of TEEs.

bandwidth of 30 kHz to examine the combinations of *S*-burst, TEE and *N*-burst in detail. The duration time of this *S*-*N* burst is 0.12 sec. The dynamic spectrum (panel (a)) shows an effect of the polarization switching signature. The thick and thin bars marked on the top of this panel indicates the polarization status of RH and LH switched alternatively. In the panel (b), temporal variations of the center frequency of the emissions are indicated by open circles, triangles, and inverse triangles respectively for the *S*-burst, the *N*-burst, and the TEE. Curves in this figure indicates trends of these bursts by using polynomial functions. The temporal variations of drift rate and band width of the emissions are also indicated in the panel (c) and (d), where drift rates are calculated from the fitted curves shown in panel (b). As can be seen in the panel (c), the drift rate of the TEE decreases gradually, and finally, merges into the trend of *N*-burst. The drift rate of *S*-burst versus time, on the other hand, keeps almost a constant value. In the panel (d), it is shown that the band widths of *S*-burst and *N*-burst keep almost constant values, while the band width of TEE rapidly increases during the first 0.05 sec and then gradually increases; and finally, the band width of TEE becomes almost the same as that of *N*-burst at the merging point. At this merging point, the center frequency, bandwidth, and drift rate of the TEE is smoothly connected to those of the *N*-burst. Figure 8 shows an example case, however, the same results can be found generally in the dynamic spectra of the *S*-*N* burst. A significant point in the result of the present analysis is that the trend of the TEE is connected to the *N*-burst smoothly at the merging point. This evidence seems to be contradictory to the argument of Riihimaa and Carr (1981) who proposed that the TEE is another trend of the *S*-burst which has a different frequency drift rate. If the TEE essentially posses a nature of the *S*-burst as suggested by Riihimaa and Carr (1981), it is difficult to explain the characteristics of the TEE at the merging point with *N*-burst. On the basis of the present study on the behavior of TEEs and *N*-bursts, it can be suggested that the TEE phenomenon does not belongs to the category of the *S*-bursts, but belongs to the category of the *N*-bursts.

4. Origin of Trailing Edge

The result of the present data analysis of *S*-*N* burst shows that TEEs do not belong to the *S*-burst, but shows property of *N*-burst. On the other hand, since the TEEs appear only in the cases of *S*-*N* burst events, the generation process of the TEE should be related to a mechanism of the *S*-burst. To identify the origin of TEEs, we have investigated various parameters to characterize the TEEs in the dynamic spectra. In Figure 9, distribution of the delay time (gap "*c*" in Figure 2) is shown in a form of a histogram. Although there are ambiguity of 17 millisecond due to the influence of the instrument switching polarization, TEEs are generated with delay times of a few tens of milliseconds. TEEs don't appear before the appearance of *S*-bursts.

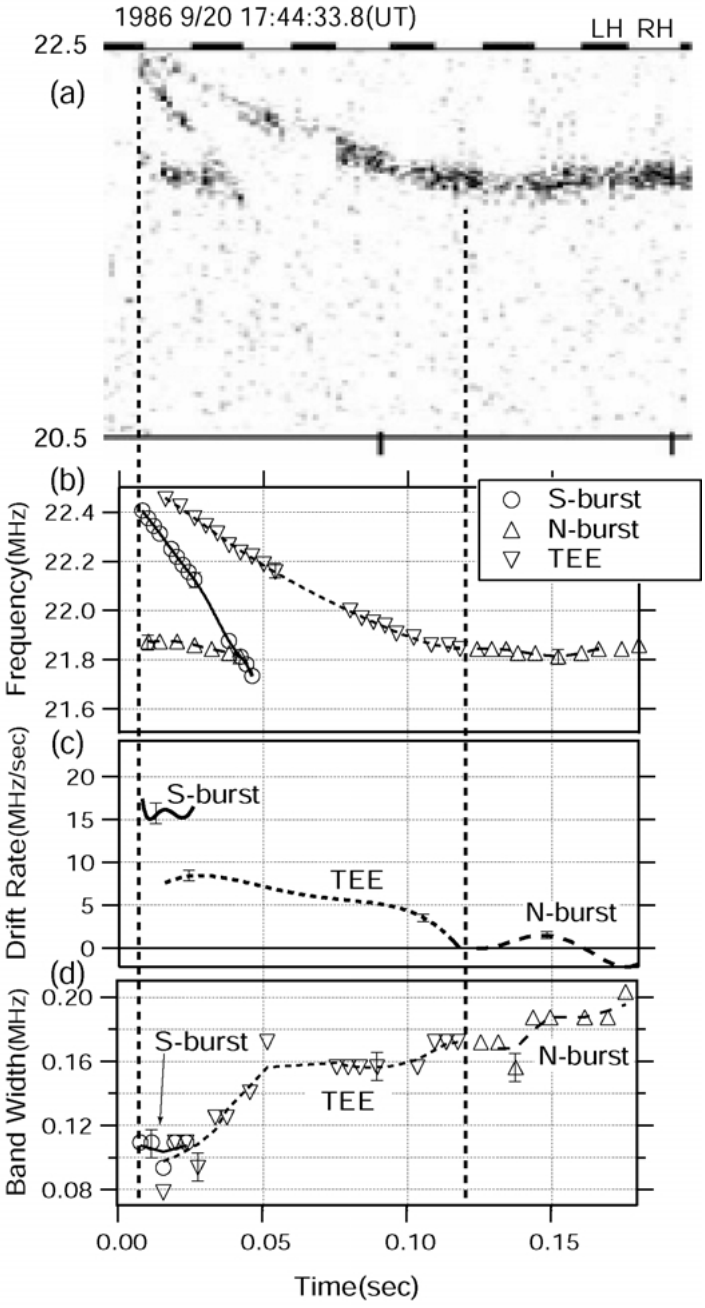

Figure 8. Properties of the micro structures of *S-N* burst. (a) A dynamic spectrum of micro structures of *S-N* burst. (b)–(d) The temporal variations of the center frequency, the drift rate, and the bandwidth.

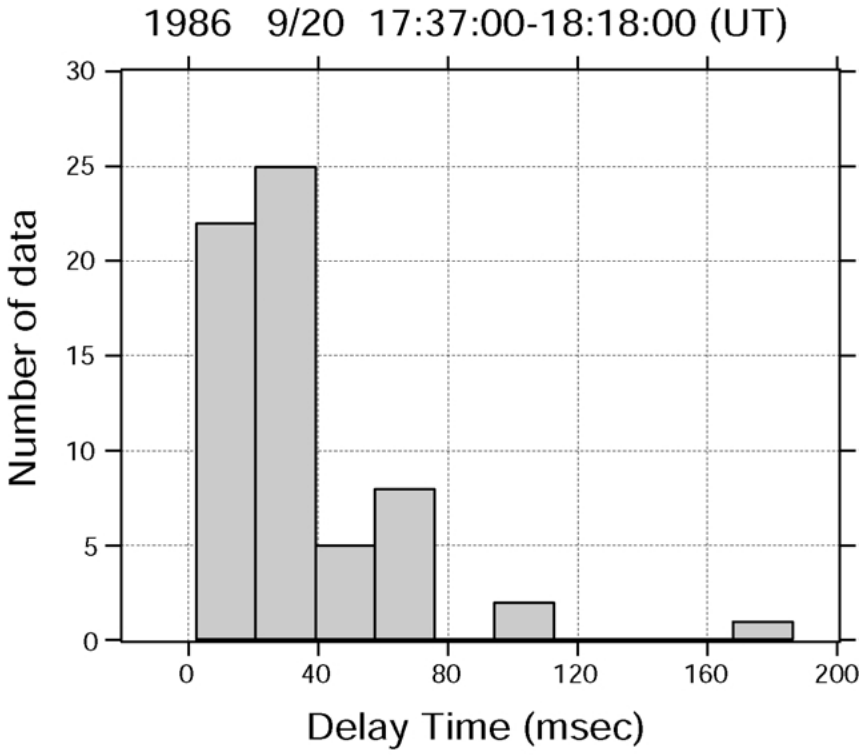

Figure 9. Distribution of the delay time from the appearance of *S*-burst.

Considering these evidences, it can be suggested that the TEE is triggered by the formation of electron cloud moving upward from the Jovian ionosphere generating the *S*-bursts. Further information on the relation between the *S*-bursts and the TEEs is obtained from the frequency range of *S*-bursts (see Figure 2). In Figure 10, relations of the "emission gaps" ("*e*" in Figure 2) versus "frequency range" ("*d*" in Figure 2) are plotted. We can see a positive correlation between the "emission gap" and the "frequency range". This result shows a possibility that the "emission gap" of the *N*-bursts is controlled by the "frequency range" of the *S*-burst. It suggests that both the TEE and the associated *S*-burst emission are started from common region simultaneously. This fact also implies that the generation regions of the TEEs and the associated *S*-bursts are both created simultaneously in the Io flux tube through an interaction process. For eliminating an ambiguity caused by the *S*-burst drift rate, the "duration time of phenomenon" ("*f*" in Figure 2) is compared with the "frequency range" of *S*-burst in Figure 11. The drift rates of the TEEs are also indicated by the gray scale for each *S*-*N* burst events. It is obvious that there is more definite positive correlation between these two parameters, and that "the duration time" is also controlled by the frequency drift rate of TEE as we can see in the tendency of the gray code in the figure. A linear solid line superimposed on the

data indicate a relation estimated from the assumption that both TEEs and *S*-bursts are started from a common origin in the formations of their generation regions. The generation region of the TEEs, however, does not radiate electromagnetic waves at the beginning of formation. Electromagnetic emissions are generated after a few tens of milliseconds from the formation of TEE region.

5. Discussions

5.1. Models for generation of *S-N* bursts

5.1.1. *Previous Interpretation*

Since *S-N* burst is not observed frequently, there are a few studies on the origin of *S-N* bursts. Riihimaa and Carr (1981) and Riihimaa (1990, 1991) proposed a mechanism that *S-N* bursts are formed by two trends of *S*-bursts interacting with *N*-bursts; two trends of *S*-bursts were thought to be originated from the same region taking different drift rate. They called these two *S*-bursts as "tilted-*V* event", and the emission gap in the *N*-bursts as "shadow event". Staelin and Rosenkranz (1982) have given a generation mechanism of the tilted-*V* event that it is generated by a velocity modulation of the electron beam. They thought that high density region created in the electron beam (they called "cusps"), which are caused by the velocity modulation, is responsible for the generation of the *S*-burst. They pointed out that the generation of two cusps in the electron beam is the origin of these two trends of *S*-bursts. However, there has been no clear explanation about the cause of the "gap" in the *N*-burst between two *S*-bursts.

5.1.2. *Present Interpretation*

As has already been discussed in the previous sections, our observation results are not in favor of the former works, especially on the origin of the TEE. If two *S*-bursts are produced by a velocity-modulation in the electron beam, there should be a correlation in the drift rate of two *S*-bursts. The statistic analyses of the present study, however, indicate that there is no correlation between the drift rates of two trends of emissions which are identified as *S*-burst and TEE. The important thing pointed out in this paper is that TEE is more likely to be a part of the *N*-burst having a slow negative frequency drift. Furthermore, TEEs and *S*-bursts are shown to be originated in a common region (see an illustration of f-t diagram given in Figure 12). A significant point revealed from the present study is that the properties of the TEEs are essentially identical with the *N*-burst for their center frequency, bandwidth and the drift rate which are continuously connected from the TEE to the *N*-burst at the merging point. In this case, frequency drift rate of the TEE is quite independent of that of the *S*-burst. On the basis of these evidences, we can state that the TEE phenomena are not in the category of *S*-bursts but belong to the category of *N*-burst. When we investigate the dynamic spectra more carefully,

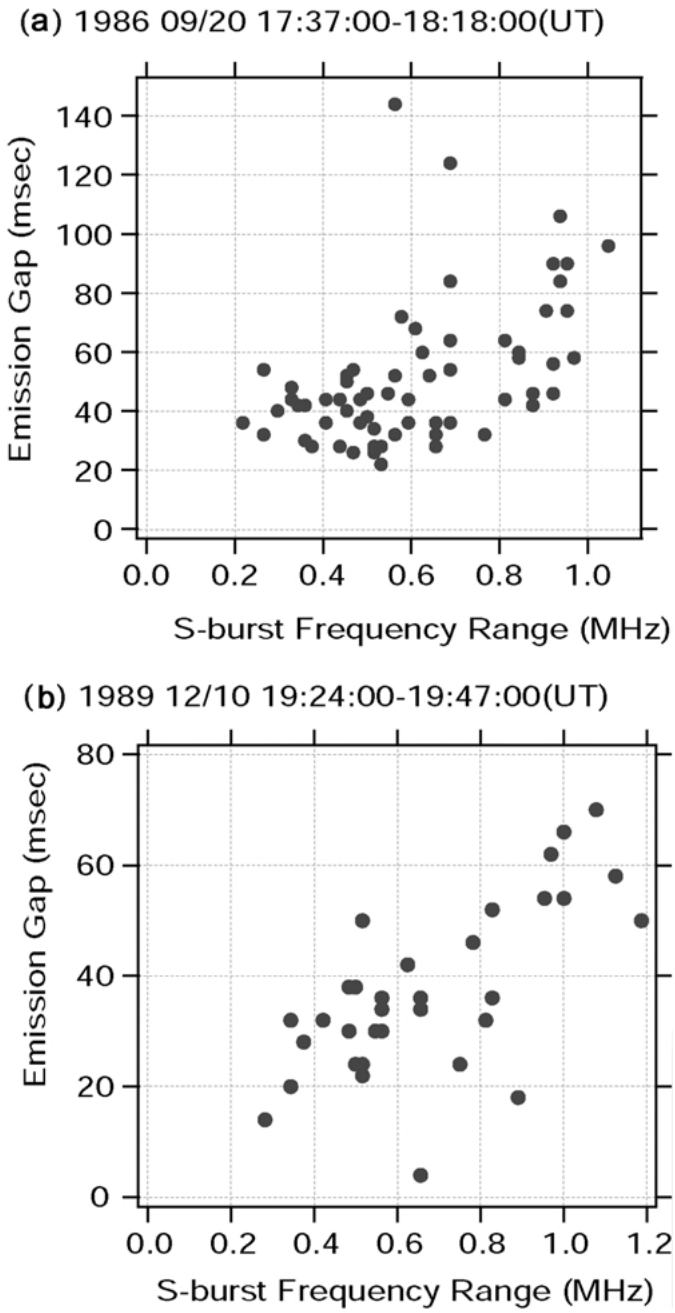

Figure 10. The "emission gaps" are plotted as a function of the "frequency range" of the *S*-burst. (a) The event observed around 18h0m (UT) on 20 September 1986. (b) The event observed around 19h30m (UT) on 10 December 1989.

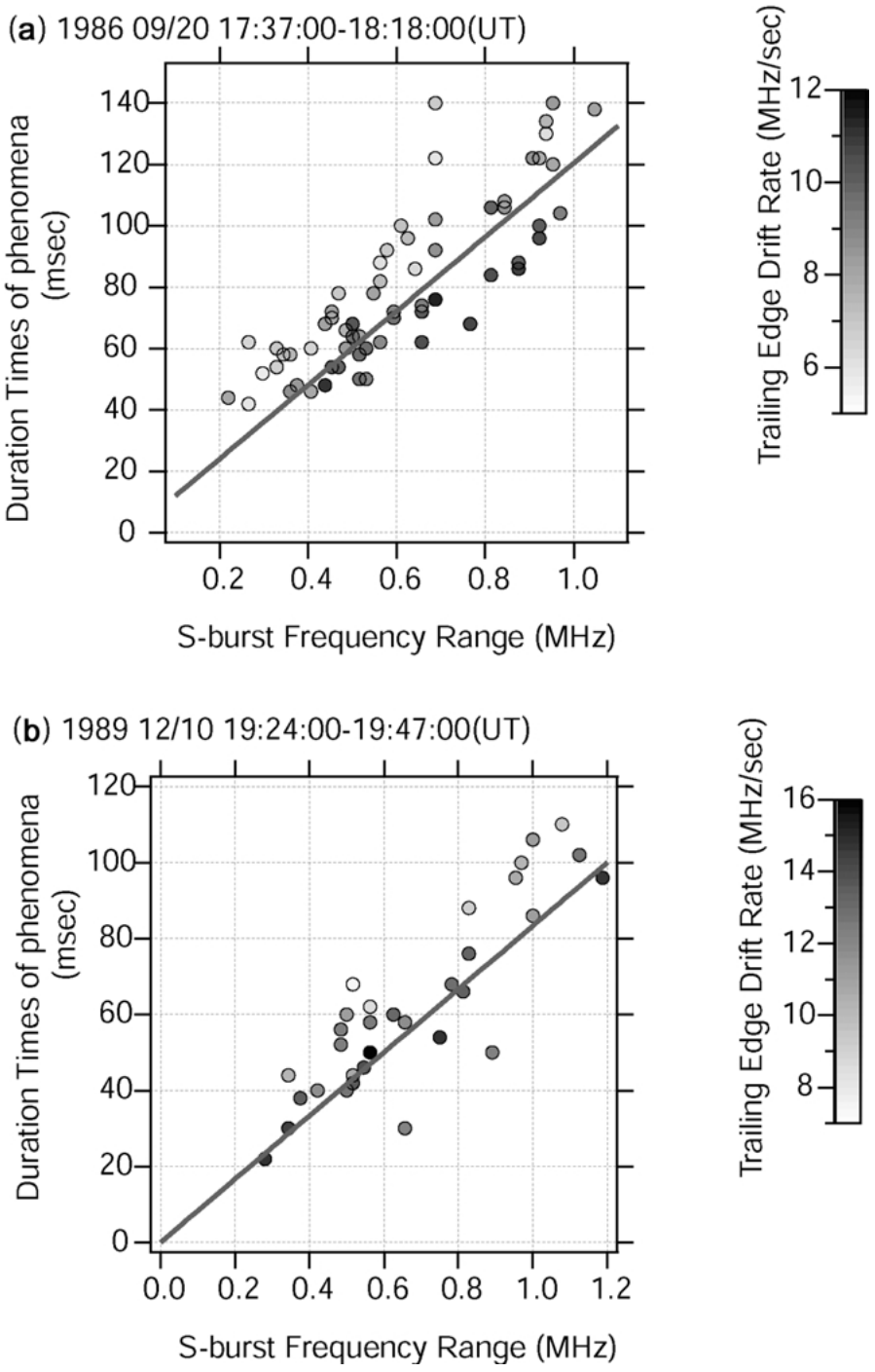

Figure 11. The "duration time of phenomena" are plotted as a function of the "frequency range" of the *S*-burst for the same events as Figure 10.

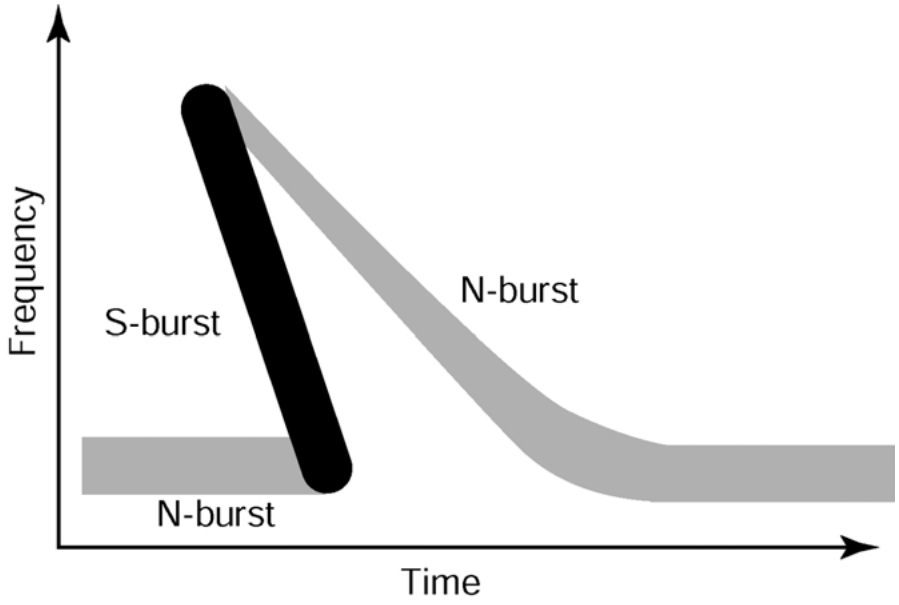

Figure 12. An illustration of the structure of *S*-*N* burst which is determined by the result of the present study.

there are examples of the TEEs that kept a constant frequency at starting time of the *S*-bursts for a moment as have been shown in Figure 13. In these cases, the frequency of *N*-bursts takes a constant value close to the start frequency of the *S*-burst, then after a few tens of msec, the TEE frequency started gradual falling tone variation (see the panels (b) and (d) in Figure 13). These TEE phenomena can not be explained by the twin *S*-bursts.

5.2. THE DISTRIBUTION OF THE ACCELERATION REGION OF ELECTRONS FOR *S*-BURSTS

The observed frequency range shows that *S*-burst is restricted within a few MHz frequency range that corresponds a few thousands km of distance for the traveling electrons along the magnetic field line. A possible model was proposed by Ellis (1982) and Zarka (1998) to explain the limited frequency range observed for the *S*-bursts. To explain the observational facts, a thin emission cone is required sweeping the direction of the observer. They estimated the thickness of the emission cone to be about 0.5° (Ellis, 1982) or about 2° (Zarka, 1998).

Our present observation results, however, can not support their interpretations. Considering the evidence that the apparitions of *S*-burst and *N*-burst occur at the same time and at the same frequency, it is not likely to state that the occurrence of the *S*-bursts is controlled by such a geometrical effects. As a consequence of this

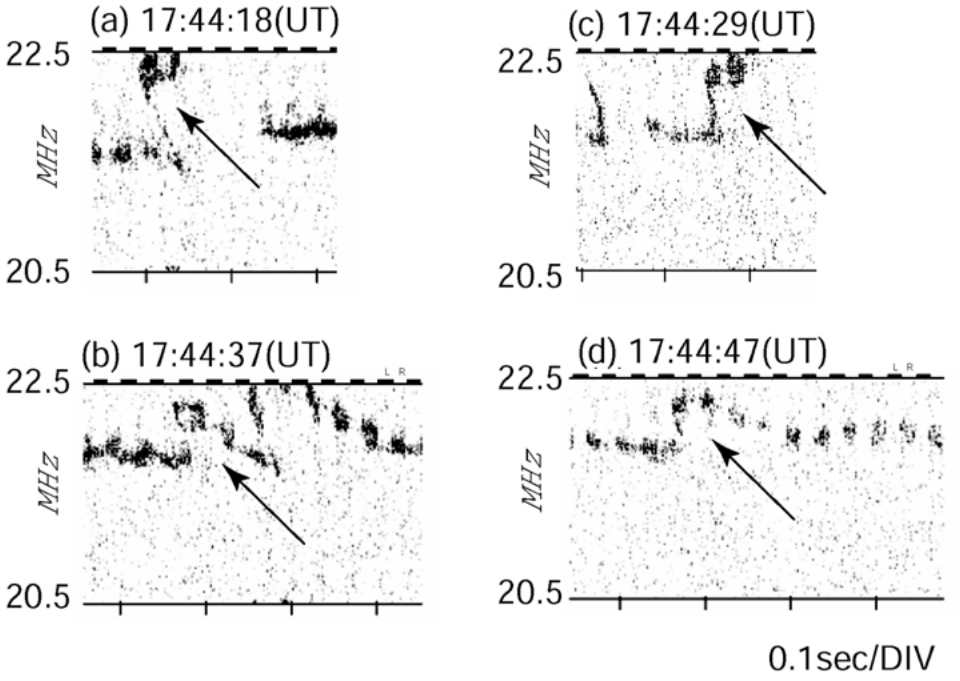

Figure 13. The examples of complicated interaction *S-N* burst (indicated by arrows) observed on 20 September 1986.

study, the apparition of *S*-burst in the dynamic spectra, then, does not reflect the geometrical relation between the source and the observer, but corresponds to the formation of electrons' cloud and generation electromagnetic waves. Furthermore, on the bases of the point that the *S*-burst and the associated TEE have a common origin, the generation of the *S*-burst can not be considered separately from the existence of the associated TEE.

Therefore, we suggest that the acceleration mechanism of bunched electrons that are responsible for the generation of the *S*-bursts is intimately related to the formation process of the electrons which generate the *N*-bursts. The frequency range of the *S*-bursts from 5 MHz to 38 MHz corresponds to the altitude range of the source positions from a few thousands km to 30,000 km assuming that the radiations take place at the local electron cyclotron frequencies. The acceleration region of the bunched electrons are thought to be distributed in this altitude range along the Io flux tube. The frequency range of each emission is a few MHz, so that the spatial extent of the source region is a few thousands km. The parallel velocities of bunched electrons with a speed in a ranges from 0.06c (0.9 keV) (*c*: light velocity) to 0.13c (4.1 keV) give a good agreement with the observed frequency drift rates. Summarizing the results of the present study as illustrated by Figure 14, the region of *N*-bursts locates and persists for a entire period of the

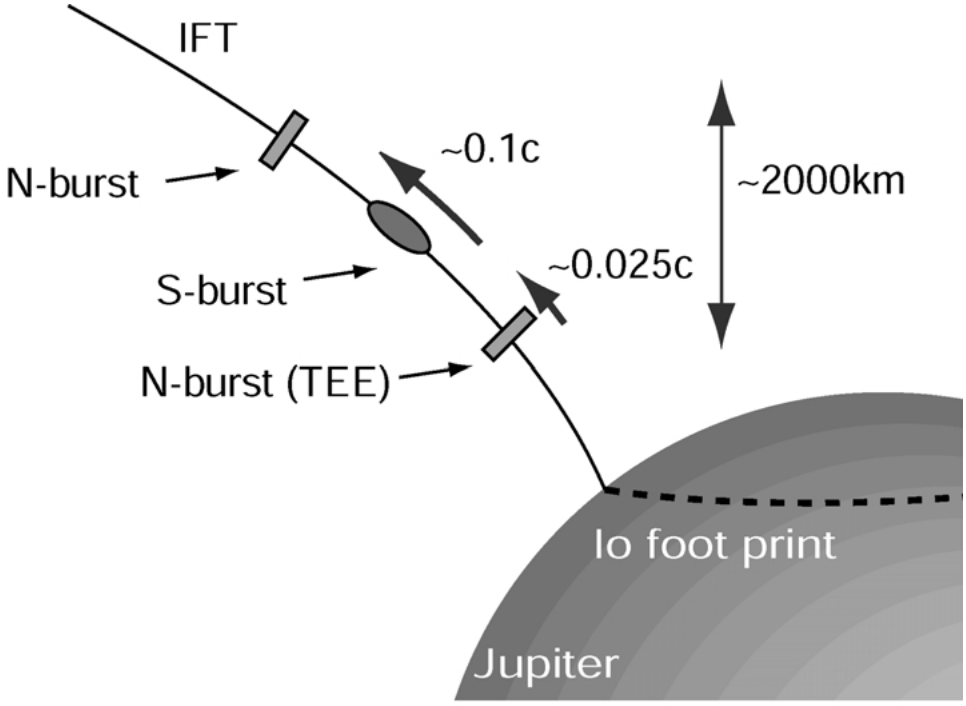

Figure 14. The relation of positions of the source regions along the magnetic field line in the *S*-*N* burst events. The source region of *S*-burst electrons is located between two source regions of *N*-bursts. The source regions of *S*-burst and TEE move upward with different velocities for about 2,000 km.

event except for the intermittent moment of the *S*-burst encounter. At the start time of TEE phenomena, a new region of *N*-burst is generated moving upward, at the same time, the formation of bunched electrons takes place that moves with a high speed of about 0.1c. Then, the high speed bunched electrons merges with the region of the *N*-burst in the highest altitude; this entry of the bunched electrons into the *N*-burst region causes the disappearance of the *N*-burst. Meanwhile, the new *N*-burst region of TEE moves up gradually, until it reaches the level of the original source region of the *N*-burst.

The physical process of the source region of *N*-burst is not understood yet. Flagg et al. (1976) supposed a generation mechanism of the *N*-burst as the coherent cyclotron mechanism, however, they have not clarified in detail. In the present study, as illustrated in Figure 14, it has been shown that the formation of a new *N*-burst source region takes place creating a TEE in lower altitude ionosphere where *S*-burst electrons are most likely to be formed. Therefore, it may be suggested that the generation region of the *N*-burst contains the parallel electric field which accelerates the bunched electrons for the *S*-burst.

In the present study we may not go into a detailed point for formation of the parallel electric field but observed evidences show that the localized parallel electric fields apparently appear along the magnetic field line in the *S*-*N* burst event. In the *S*-*N* burst events, two kinds of potential drops seems to appear in the Io flux tube. One potential drop is created first at a high altitude which forms the generation region of the quasi steady *N*-burst. And then, at lower altitude, the other potential drop appears suddenly, and the bunched electrons for the *S*-burst is accelerated by this electric field. Because the bandwidth of the TEE is narrower than 100 kHz, the spacial extent of the acceleration region of *S*-burst electrons along the magnetic field line is very thin, with a width less than 100 km.

It is also an interesting subject that the original *N*-bursts disappear when the *S*-bursts merge with the *N*-burst. It seems to happen at the moment when the *S*-burst electrons arrive at the source region of the original *N*-bursts. We can suggest several possibilities for this destruction processes of the source region of *N*-burst. One of such processes is a merge of the beam electrons of *S*-bursts with the positive charge regions of the double layer type electric field which generates *N*-bursts. The sudden neutralization by the arriving beam electrons of *S*-bursts may become an origin of strong instabilities which causes the destruction of the *N*-burst source region. Then, the potential drop disappears until the second potential drop moves up to the original point. The potential drop in the lower altitude is rather unstable and start to move up with a fairly fast speed, though it is relatively slow speed compared with the *S*-bursts electrons. Of course, in a present stage of the study such a scenario is one of the possibilities and further observational studies are required to determine the *N*-bursts as well as *S*-bursts.

6. Conclusion

To seek the generation mechanism of the *S*-burst and the related emissions in the Io-B region of the Jovian decametric radiation (DAM), characteristics of the *S*-bursts and the *S*-*N* bursts, have been investigated by analyzing the data obtained by the dynamic spectrograph with the high-time resolution in a period from 1983 to 2000. Parameters which represent the characteristics of the *S*-*N* bursts phenomena have been analyzed to clarify whether the Trailing Edge Emissions (TEEs) possess the same nature of the *S*-bursts or not. From the analyses of the microscopic view of the dynamic spectra, the following properties of the *S*-*N* bursts are found: (1) There is no correlation between the drift rates of the *S*-burst and the associated TEE. (2) The velocity range of the motion of TEE is narrower than that of the *S*-burst in each event. (3) The TEE phenomena show a nature to be smoothly connected to the *N*-burst in the dynamic spectra reflecting the fact that the center frequency, bandwidth and the drift rate of the TEE coincide with these of the *N*-burst at the merging point, and (4) The drift rate of the *S*-burst clearly depend on the frequency while there is no distinct frequency dependence for the drift rate of the TEE. There results

suggest that TEE is not a kind of *S*-bursts but a part of the *N*- bursts. Furthermore, the results of the correlation analysis between the "*S*-burst frequency range" and the "*S*-*N* burst duration time" clearly indicate that the TEE and the *S*-burst start from the common region at the same time. On the basis of these facts, we can conclude that the occurrence of the *S*-burst in the dynamic spectra is not controlled by the geometrical effect between the direction of the emissions and observers, but rather show the generation of the source regions at the moment. The acceleration regions of the bunched electrons which is responsible for the *S*-burst event, are not located near the Jovian ionosphere nor close to the Io satellite, but distributed in a wide altitude range from a few thousands km to 30,000 km above the Jovian ionosphere. As the results of the present study, a new scenario has been proposed to explain the *S*-*N* bursts of Jovian Decameter emissions that reveals dynamic features of acceleration and motion of bunched electrons formed in the Io flux tube. The origin of this unique process of plasma physics in Jupiter will take a important role for the understanding of electromagnetic process of the fast rotating magnetized planet, and will be further extended to the understanding of pulsers.

References

Boudjada, M. Y., Galopeau, P. H. M., and Rucker, H. O.: 1996, 'A Discussion on the *S*-Burst Drift Model', *Astron. Astrophys.* **306**, L9–L12.

Boudjada, M. Y., Rucker, H. O., Ladreiter, H. P., and Ryabov, B. P.: 1995, 'Jovian *S*-Bursts: The Event of 4 January', *Astron. Astrophys.* **295**, 782–794.

Carr, T. D., Desch, M. D., and Alexander, J. K.: 1983, 'Phenomenology of Magnetospheric Radio Emissions', in *Physics of the Jovian Magnetosphere*, Cambridge University Press, pp. 226–284.

Desch, M. D., Flagg, R. S., and May, J.: 1978, 'Jovian *S*-Burst Observations at 32 MHz', *Nature* **272**, 38–40.

Ellis, G. R. A.: 1975, 'Spectra of the Jupiter Radio Bursts', *Nature* **253**, 415–417.

Ellis, G. R. A.: 1982, 'Observations of the Jupiter *S*-Bursts between 3-2 and 32 MHz', *Aust. J. Phys.* **35**, 165–175.

Flagg, R. S. and Desch, M. D.: 1979, 'Simultaneous Multifrequency Observations of Jovian S Bursts', *J. Geophys. Res.* **84**(A8), 4,238–4,244.

Flagg, R. S., Krausche, D. S., and Lebo, G. R.: 1976, 'High Resolution Spectra Analysis of the Jovian Decametric Radiation. II. The Band-Like Emissions', *Icarus* **29**, 477–482.

Krausche, D. S., Flagg, R. S., Lebo, G. R., and Smith, A. G.: 1976, 'High Resolution Spectral Analyses of the Jovian Decametric Radiation. I. Burst Morphology and Drift Rates', *Icarus* **29**, 463–475.

Leblanc, Y. and Rubio, Y.: 1982, 'A Narrow-Band Splitting at the Jovian Decametric Cutoff Frequency', *Astron. Astrophys.* **111**, 284–294.

Leblanc, Y., Genova, F., and de la Noë, J.: 1980a, 'The Jovian *S*-Bursts: I. Occurrence with *L*-Bursts and Frequency Limit', *Astron. Astrophys.* **86**, 342–348.

Leblanc, Y., Aubier, M., Rosolen, C., Genova, F., and de la Noë, J.: 1980b, 'The Jovian *S*-Bursts: Frequency Drift Measurements at Different Frequencies throughout Several Storms', *Astron. Astrophys.* 86: 349–354.

Riihimaa, J. J.: 1964, High-Resolution Spectral Observations of Jupiter's Decametric Radio Emission', *Nature* **202**, 476–477.

Riihimaa, J. J.: 1970, 'Modulation Lanes in the Dynamic Spectra of Jovian L Bursts', *Astron. Astrophys.* **4**, 180–188.

Riihimaa, J. J.: 1977, *S*-Burst in Jupiter's Decametric Radio Spectra', *Astrophys. Space Sci.* **51**, 363–383.

Riihimaa, J. J.: 1978, '*L*-Bursts in Jupiter's Decametric Radio Spectra', *Astrophys. Space Sci.* **56**, 503–518.

Riihimaa, J. J.: 1979, 'Drift Rates of Jupiter's *S*-Bursts', *Nature* **279**, 783–785.

Riihimaa, J. J.: 1985, 'Bursts of Type N in the Jupiter's Decametric Radio Spectra', *Earth Moon Planets* **32**, 9–19.

Riihimaa, J. J.: 1990, 'Variants of Tilted-V Events in Jupiter's Decametric Radio Spectra', *Earth Moon Planets* **48**, 49–54.

Riihimaa, J. J.: 1991, 'Evolution of the Spectral Fine Structure of Jupiter's Decametric *S*-Storms', *Earth Moon Planets* **53**, 157–182.

Riihimaa, J. J. and Carr, T. D.: 1981, 'Interaction of S- and *L*-Bursts in Jupiter's Decametric Radio Spectra', *Moon Planets* **25**, 373–387.

Staelin, D. H. and Rosenkranz, P. W.: 1982, 'Formation of Jovian Decametric *S* Bursts by Modulated Electron Streams', *J. Geophys. Res.* **87**(A12), 10,401–10,406.

Warwick, J. W.: 1963, 'Dynamic Spectra of Jupiter's Decametric Emission, 1961', *Astrophys. J.* **137**, 41–60.

Warwick, J. W. and Gordon, M. A.: 1965, 'Frequency and Polarization Structure of Jupiter's Decametric Emission on a 10-Millisecond Scale', *Radio Sci.* **69D**, 1,537–1,542.

Zarka, P.: 1998, 'Auroral Radio Emissions at the Outer Planets: Observations and Theories', *J. Geophys. Res. Lett.* **103**, 2,0159–2,0194.

Zarka, P., Farges, T., Ryabov, Boris P., and Abada-Simon, M.: 1996, 'A Scenario for Jovian *S*-Bursts', *Geophys. Res. Lett.* **23**, 125–128.